J. Fluid Mech. (2014), *vol.* 739, *pp.* 363–391. © Cambridge University Press 2013
doi:10.1017/jfm.2013.615

Behaviour of rarefied gas flow near the junction of a suddenly expanding tube

Vijay Varade[1], Amit Agrawal[2,†] and A. M. Pradeep[3]

[1]Centre for Research in Nanotechnology and Science, Indian Institute of Technology Bombay, Mumbai, 400076, India

[2]Department of Mechanical Engineering, Indian Institute of Technology Bombay, Mumbai, 400076, India

[3]Department of Aerospace Engineering, Indian Institute of Technology Bombay, Mumbai, 400076, India

(Received 28 April 2013; revised 4 November 2013; accepted 14 November 2013;
first published online 18 December 2013)

This paper presents an experimental study of isothermal rarefied gas flow through a tube with sudden expansion in the slip flow regime. The measurements reported here are for nitrogen flowing at low pressures in conventional tubes with sudden expansion area ratios of 1.48, 3.74, 12.43 and 64. The flow is dynamically similar to gas flow in a microchannel as the Knudsen number ($0.0001 < Kn < 0.075$) falls in the slip flow regime; the Reynolds number in the smaller section (Re_s) ranges between 0.2 and 837. The static pressure along the wall is measured for different mass flow rates controlled by a mass flow controller and analysed to understand the flow behaviour. The velocity profiles are obtained through a momentum balance and using the pressure measurements. A discontinuity in the slope of pressure at the sudden expansion junction is noted and given special attention. The absence of flow separation is another key feature observed from the measurements. The streamlines are found to be concave near the junction. It is demonstrated that the flow 'senses' the oncoming sudden expansion junction and starts adjusting itself much before reaching the junction; this interesting behaviour is attributed to an increased axial momentum diffusion and wall slip. The additional acceleration of the central core of the gas flow causes an increase in the wall shear stress and a larger pressure drop as compared with a straight tube. These results are not previously available and should help in improving understanding of gaseous slip flows.

Key words: micro-/nano-fluid dynamics, non-continuum effects, rarefied gas flow

1. Introduction

Flow through a microchannel is of great interest and has been investigated in the recent past. The majority of the studies however were on straight microchannels. For example, analytical investigations on gas flow through a straight microchannel is available in Harley *et al.* (1995), Arkilic, Schimidt & Breuer (1997) and Dongari, Agrawal & Agrawal (2007) in the slip regime; and Singh, Dongari & Agrawal (2013) in the transition regime. The experimental studies on gas flow through straight microchannels are reported by Pong *et al.* (1994), Harley *et al.* (1995), Arkilic *et al.* (1997), Zohar *et al.* (2002), Ewart *et al.* (2006, 2007), Vijayalakshmi *et al.* (2009) and

† Email address for correspondence: amit.agrawal@iitb.ac.in

Pitakarnnop *et al.* (2010). Numerical simulation results are available in the work of Agrawal & Agrawal (2006) and Roohi & Darbandi (2009), among others. Gas flow through a microtube is discussed by Weng, Li & Hwang (1999), Morini, Lorenzini & Salvigni (2006), Verma *et al.* (2009), Yamaguchi *et al.* (2011) and Yang *et al.* (2012). An extensive, numerical and analytical study on rarefied gas flows through a capillary was reported by Sharipov & Seleznev (1998); this extensive review can be referred to for rarefied gas flow studies conducted prior to 1998. Sreekanth (1969) and Demsis *et al.* (2009) and Demsis, Prabhu & Agrawal (2010) presented experimental investigations on gas flow through conventional tubes under rarefied conditions, with the flow being dynamically similar to gas flow in a microchannel. A recent and comprehensive review on gas flow in a microchannel was given by Agrawal (2011). However, in practical applications, a microchannel is unlikely to be straight. Bends, bifurcations, junctions, expansions and contractions are some common features of microsystems and characterization of the flow behaviour through such sections is of both practical and fundamental interest. The present work focuses on experimental investigation of the flow behaviour of isothermal rarefied gas flow through a tube with sudden expansion in the slip flow regime.

There are studies on sudden expansion in the continuum regime for incompressible flow through circular/non-circular passages involving Newtonian fluid. In a computational work by Macagno & Hung (1967), a small corner eddy was noted for viscous liquid flow through a circular conduit sudden expansion at a low Reynolds number ($Re_s = 1$, on the basis of the smaller tube). Durst, Melling & Whitelaw (1974) experimentally investigated air flow through a plane symmetric sudden expansion duct. Flow separation was observed adjacent to the sudden expansion step. The effect of Reynolds number on the frequency, amplitude and spatial occurrence of flow pulsation at the junction was analysed. It was noted that the flow is stable at a low Reynolds number ($Re = 56$) whereas the flow becomes less stable at higher Reynolds numbers. Oliveira & Pinho (1997) noted flow separation at $Re_s = 12.5$ in a numerical analysis for an area ratio of 2.6 involving liquid flow. In an experimental work on laminar liquid flow through axisymmetric sudden expansion by Hammad, Otugen & Arik (1999), it was noted that the recirculating eddy strength increases nonlinearly with increasing Reynolds number. Sisawath *et al.* (2002) proposed an approximation for the excess pressure drop due to sudden expansion in a pipe. Chalfi & Ghiaasiaan (2008) measured pressure drop for air and water flow (Re_s 160–11 000) through a sudden expansion test section. Goharzadeh & Rodgers (2009) experimentally observed recirculating regions for laminar liquid flow through a sudden inward expansion within a confined annular geometry. A numerical analysis of axisymmetric planar sudden expansion laminar flow for an incompressible fluid was presented by Dagtekin & Unsal (2011). The effect on the relative eddy intensity, location of the eddy centre and eddy reattachment length was investigated in their work.

The investigations on *incompressible* flow through a microchannel with expansion are however limited. Pan *et al.* (2004) experimentally observed flow separation at the junction for liquid flow through a microchannel with a sudden expansion. The pressure drop caused by continuum air and water flow ($1000 < Re < 7000$) through sudden expansion in a microtube was experimentally investigated by Abdelall *et al.* (2005). It was reported that the expansion and contraction loss coefficients are different for air and water flows. The experimental results of Tsai *et al.* (2007) with liquid flow indicated that a flow separation vortex forms at the sudden expansion corner in a microchannel with a high aspect ratio. A recent experimental study on liquid flow through a continuously expanding microchannel by Duryodhan, Singh & Agrawal (2013) indicated that flow separation occurs beyond a critical divergence angle of 16°,

which agrees with the corresponding value for continuum flow. It can be noted from the above studies that certain key features such as flow separation, secondary flow and flow reattachment are observed for laminar, incompressible flow (even for very low Reynolds number) through expansion. Similar behaviour applies for liquid flow at the microscale; the behaviour of gas may however be different as reviewed next.

An experimental study on rarefied gas flow ($Kn = 0.0026$–1.75, nitrogen) through a circular tube with sudden increase in cross-sectional area was presented by Rathakrishnan & Sreekanth (1995). They highlighted the 'relief effect' whereby a considerable increase in the flow rate (as compared with a corresponding straight tube) occurs due to a sudden increase in the cross-sectional area, at all levels of inlet pressures. It was noted that in the transition regime, the pressure ratio and the length-to-diameter ratio of the passage have a major influence on the discharge through sudden enlargements. Lee, Wong & Zohar (2002) experimentally investigated gas flows through microchannels connected through a transition section with included angle varying from 5 to 180° using nitrogen gas. They observed that the measured mass flow rate decreases and the pressure loss increases with increasing included angle of the transition section. Agrawal, Djenidi & Antonia (2005) performed two-dimensional simulations based on isothermal lattice Boltzmann method for a microchannel with a sudden expansion. The absence of recirculating fluid near the junction was noted from their simulation results. The direct simulation Monte Carlo (DSMC) method was used by Xue & Chen (2003) for simulation of rarefied gas (nitrogen) flow in the slip and transition regimes ($0.008 < Kn < 10$) through a micro-backward-facing step. A nonlinear pressure distribution was noted before and after the step. The flow acceleration up to the sudden expansion step and sudden jump in the velocity at the step was reported by them. Xue & Chen (2003) reported that the flow separation disappears completely in the transition regime ($Kn > 0.1$). Celik & Edis (2007) used a characteristic-based split Navier–Stokes finite-element method (FEM) solver for simulation of micro-backward-facing step duct flow in the slip regime. A recirculation region behind the step was noted by them. The DSMC simulation for rarefied gas flow in the slip and transition regimes over a backward facing step was also reported by Kursun & Kapat (2007).

It is noted that even in the continuum regime, the number of studies in the *laminar* flow regime is limited. This hampers our understanding of the overall flow behaviour (and its implication, for example, on the overall pressure drop) as well as the local flow behaviour near the junction. Further, with a change of scale or introduction of the rarefaction effect, the flow behaviour near the junction needs to be better understood. The numerical analysis of Agrawal *et al.* (2005) indicated the absence of recirculatory motion near the junction, even with a large area ratio. Further, it was argued that the analysis of such a microchannel can be carried out in terms of its primary units (straight microchannel) for which theoretical results and supporting experimental data is already available. These interesting results need experimental verification, which provided the motivation for the present work.

This paper presents an experimental study on isothermal rarefied gas flow through a tube with sudden expansion in the slip flow regime using nitrogen as the working fluid. The approach of Sreekanth (1969) and Demsis *et al.* (2009, 2010) is also followed here, which has the advantage of providing detailed local information without the difficulty of having to perform measurements at micrometre scales. The objectives of this work are to investigate the gas microflow behaviour through a sudden expansion and to highlight significant differences with respect to continuum behaviour. The static pressure variation along the wall is measured and analysed to understand the flow behaviour. The velocity profile is obtained indirectly from static pressure

Parameter	Maximum uncertainty
Mass flow rate	±2 % of full scale
Absolute pressure	±0.15 % of the reading
Diameter	±0.1 %
Reynolds number	±2 %
Knudsen number	±0.5 %
Pressure loss coefficient	±6 %
Temperature	±0.3 K

TABLE 1. Maximum uncertainty in various measured and derived parameters.

measurements at the wall and the mass flow rate. The effects of rarefaction and mass flow rate on the pressure loss coefficient for sudden expansion are also investigated.

2. Experimental set-up and procedure

2.1. *Vacuum system and instrumentation*

The experimental set-up consists of a vacuum system, inlet reservoir, outlet reservoir and a mass flow controller, as shown in figure 1(*a*). The vacuum system consists of a diffusion pump with a maximum pumping speed of 700 l min^{-1} and a rotary pump with a speed of 350 l min^{-1}. The maximum vacuum that can be achieved by the vacuum system is 10^{-6} mbar. An air filter is used to filter particles of size larger than 25 μm in the incoming gas stream. Three different mass flow controllers (from M/s MKS Instruments) with ranges of 0–20, 0–200 and 0–5000 sccm (standard cubic centimetres per minute) are used to achieve different Reynolds and Knudsen numbers in the experiments. The absolute pressure at the test section is measured by an absolute pressure transducer (also from M/s MKS Instruments) of range either 0–100 or 0–10 000 Pa. The uncertainties in measurement of flow rate and pressure (along with other measured and derived parameters) are tabulated in table 1. The uncertainty in mass flow rate is the combined uncertainty because of the measurement uncertainty and leakage.

2.2. *Test section*

The test section geometry with the location of the pressure measurement taps is shown in figure 1(*b*). Flush mounted (with internal wall) pressure taps (external diameter 2.2 mm, internal diameter 1.2 mm) are provided along the wall for pressure measurements. The test sections of area ratio (*AR*) 1.48 and 3.74 are provided with 13 pressure taps, while the test section of area ratio 12.34 is provided with 14 pressure taps and area ratio 64 is provided with 19 pressure taps. The first pressure tap is located at a distance greater than the largest length required for the flow to develop fully. The fully developed length is estimated from three different criteria as presented below and the most conservative estimate was utilized while designing. The same length is allowed downstream of the last pressure tap to avoid any end effects, except with the area ratio of 64 for which additional length is allowed downstream of the last pressure tap (see table 2).

Chen (1973) analysed the development length data of Friedmann, Gillis & Liron (1968) and proposed the following formula for continuum flow:

$$\frac{L_D}{D} = \frac{0.60}{0.035Re + 1} + 0.056Re \tag{2.1}$$

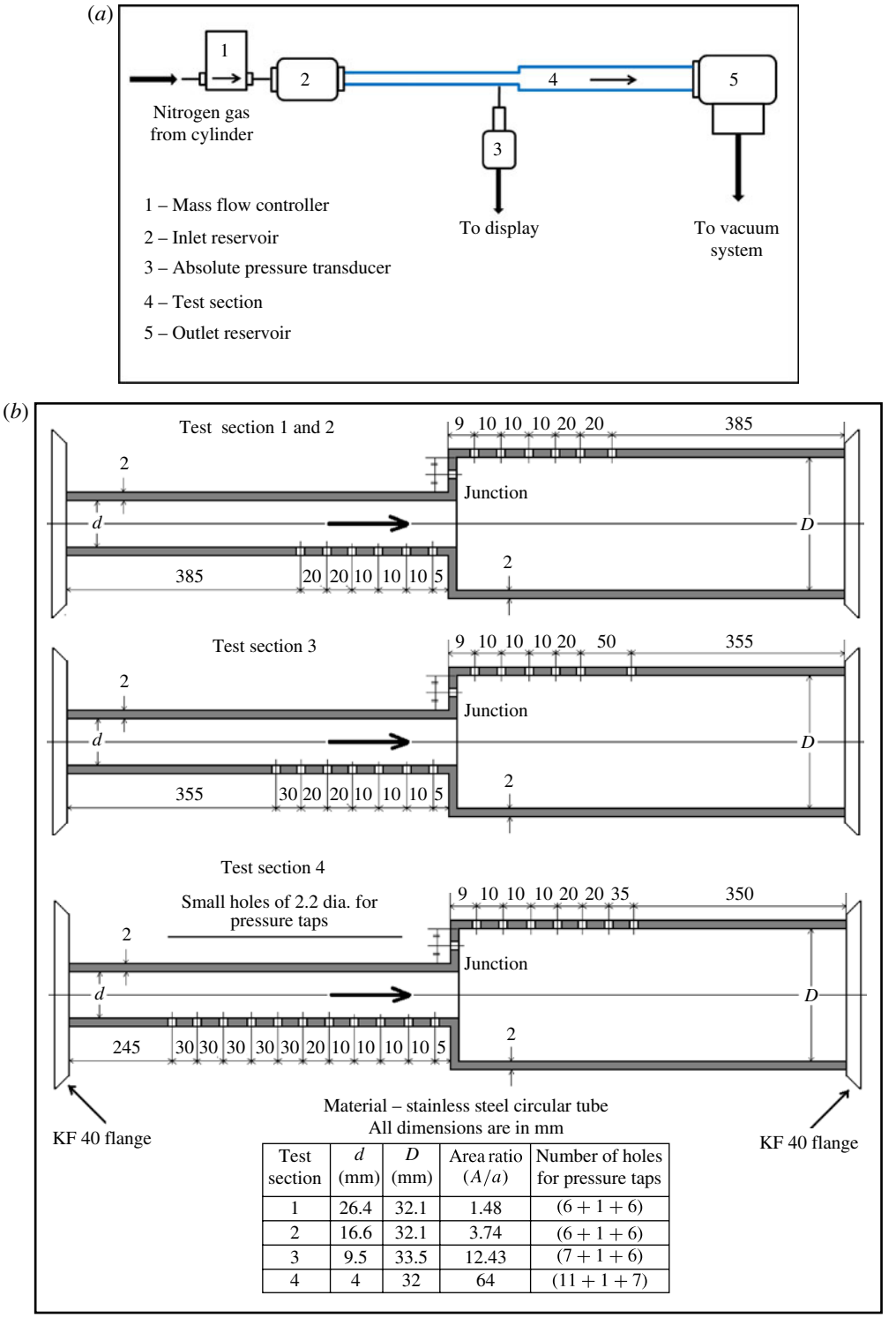

Test section	d (mm)	D (mm)	Area ratio (A/a)	Number of holes for pressure taps
1	26.4	32.1	1.48	(6 + 1 + 6)
2	16.6	32.1	3.74	(6 + 1 + 6)
3	9.5	33.5	12.43	(7 + 1 + 6)
4	4	32	64	(11 + 1 + 7)

FIGURE 1. For caption see the next page.

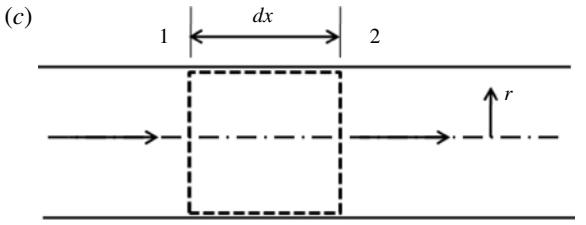

FIGURE 1. (Colour online) (cntd). (*a*) Schematic diagram of the experimental set-up. (*b*) Test section geometry for sudden expansion. (*c*) Control volume for flow through sudden expansion.

Test section	1	2	3	4
d (mm)	26.4	16.6	9.5	4
D (mm)	32.1	32.1	33.5	32
Fd_1 (mm)	385	385	355	245
L_1 (mm)	77	77	107	217
L_2 (mm)	77	77	107	112
$L(L_1 + L_2,$ mm)	154	154	214	329
Fd_2 (mm)	385	385	355	350
Area ratio ($AR = A/a$)	1.48	3.74	12.43	64
Number of pressure taps	$(6 + 1 + 6)$	$(6 + 1 + 6)$	$(7 + 1 + 6)$	$(11 + 1 + 7)$
Mass flow rate	7.49×10^{-8}–8.42×10^{-5} kg s^{-1} (4–4500 sccm)			
Re in small section (Re_s)	0.2–228	0.32–363	0.56–494	1.34–837
Kn at the inlet (Kn_i)	0.0001–0.037	0.0002–0.043	0.0005–0.045	0.0005–0.016
Kn at the junction (Kn_j)	0.0001–0.037	0.0002–0.043	0.0005–0.067	0.001–0.075
Mach number at inlet (M_i)	0.005–0.02	0.009–0.056	0.017–0.16	0.015–0.26

TABLE 2. Test conditions employed in the measurements. Here Fd_1 = flow developing length upstream of the first pressure tap, L_1 = length between the first pressure tap and the sudden expansion junction, L_2 = length between the sudden expansion junction and the last pressure tap, L = length between the first and last pressure taps and Fd_2 = flow developing length downstream of the last pressure tap.

where L_D the flow development length in metres, D is the internal diameter of the pipe in metres and Re is the Reynolds number. Dombrowski *et al.* (1993) proposed the following correlation for hydrodynamic developing length in a circular pipe:

$$\frac{L_D}{D} = 0.260 + 0.055Re + 0.379\mathrm{e}^{-0.148Re}. \tag{2.2}$$

Barber & Emerson (2001) concluded that the formulae of Chen (1973) and Dombrowski *et al.* (1993) for continuum flows are equally valid in the slip flow regime for a circular pipe. The expression for the developing length proposed by Sreekanth (1969) on the basis of experiments (in the range of $Re = 0.045$–22.57 and $Kn = 0.007$–0.24), is as follows:

$$\frac{L_D}{D} = \frac{kRe}{4} \quad (k = 0.20). \tag{2.3}$$

Area ratio	Knudsen number at the junction	Gas temperature in Kelvin		
		Inlet	Junction	Outlet
3.74	0.04	300.1	299.7	299.8
	0.0002	300.2	299.7	300.0
12.43	0.06	300.2	299.6	300.0
	0.0005	300.1	299.7	299.8
64	0.07	300.1	299.5	299.8
	0.001	300.0	299.6	299.9

TABLE 3. Gas temperature measurement.

Note that the development length employed in the measurements is larger than the maximum of the developing lengths calculated (for highest Re of the experimental range) using (2.1)–(2.3). It can therefore be concluded that the flow is fully developed at the first pressure tap location.

2.3. *Experimental procedure*

The validation of the experimental set-up is established by comparing results against those in the literature. Towards this, the pressure drop for different mass rates is noted for a straight tube. The $f\,Re$ value on the basis of these measurements are compared against the $f\,Re$ value obtained from the correlation proposed by Verma *et al.* (2009). The correlation of Verma *et al.* (2009)

$$f\,Re = \frac{64}{1 + 14.886Kn} \tag{2.4}$$

for laminar flow in a smooth circular tube was obtained using experimental data from several researchers. The deviation is observed to be less than 2 %, thereby validating the experimental set-up and data reduction procedure.

Thereafter, experiments for sudden expansion are carried out. The set-up is tested for leakage using the procedure discussed in Demsis *et al.* (2010). The leakage is ensured to be less than 2 % of the mass flow rate employed in the measurements. The absolute static pressure is measured along the wall of the test sections for different mass flow rates of nitrogen at 300 K. The temperatures of the gas at the inlet, junction and the outlet were explicitly measured as tabulated in table 3. The variation in temperature was noted to be less than 1 °C, which confirmed that the flow can be treated as isothermal. The flow Reynolds number is varied in the range 0.2–837 (Mach number at inlet $M_i = 0.005$–0.26) and the Knudsen number is varied in the range 0.0001–0.075. The Knudsen number (Sreekanth 1969; Sharipov & Seleznev 1998) and Reynolds number are calculated as

$$Kn = \frac{\lambda}{d} = \frac{\mu\sqrt{\pi RT/2}}{pd} \tag{2.5}$$

$$Re = \frac{4\dot{m}}{\pi d\mu} \tag{2.6}$$

where λ is the mean free path of molecules (m), d is the diameter of the tube (m), μ dynamic viscosity (Pa s), R is the specific gas constant (J (kg K)$^{-1}$), T is the temperature of gas (K), p is the gas pressure (Pa), $\dot{m}$ is the mass flow rate (kg s^{-1}). Note that the Knudsen numbers at both the inlet (Kn_i) and junction (Kn_j) are calculated on the basis of the smaller tube diameter of the sudden expansion as

the characteristic length. The range of test conditions employed in the measurements is tabulated in table 2. Note that the results reported in this paper are in the slip regime; performing measurements in the transition regime is beyond the scope of the current work. Our results show several novel behaviours in the slip regime; such behaviours can be explored further in the transition regime.

3. Results

The experiments are carried out for the slip ($0.001 < Kn < 0.1$) flow regime. The local pressure variation is noted and analysed. The velocity distribution is obtained theoretically using measured values of pressure and mass flow rate as discussed in § 3.3. The effect of expansion on the wall shear stress and momentum is analysed in § 3.4.

3.1. *Pressure variation along the wall*

The variation of non-dimensional static pressure along the wall is presented in figure 2 for different Knudsen numbers ($Kn_j = 0.0005$–0.04) and four area ratios. These measurements are for Re_s between 0.2 and 837. The location of the junction is marked in the figure. Figure 2(*a,b*) show that the static pressure variation is linear in both the tubes ($Kn_j \leqslant 0.004$, area ratio 1.48 and 3.74), with a higher pressure drop in the smaller tube. It can be noted from figure 2(*c,d*) (for an area ratio of 12.43) that the pressure variation passes through two different flow behaviours. The static pressure variation for $Kn_j < 0.001$ is similar to curve I in figure 2(*f*). An increase in the rarefaction at the junction ($Kn_j = 0.003$; figure 2*d*) causes an increased pressure ratio in the smaller tube, and the pressure variation resembles curve II in figure 2(*f*). For the case $Kn_j = 0.006$ in figure 2(*d*), the slope of the curve is different on the left and right sides of the junction; this discontinuity in slope is indicated as curve III in figure 2(*f*). The discontinuity in the slope at the junction becomes particularly pronounced for an area ratio of 64. Note from figure 2(*e*) that the overall pressure gradient increases with an increase in the Knudsen number. Therefore, figure 2(*d*) indicates two different flow behaviours: that is a continuous slope at the junction for low *Kn*, and a discontinuity in slope at the junction for higher values of Knudsen number.

The critical Knudsen number for transition from a continuous slope at the junction to discontinuity in the slope at the junction is plotted against area ratio in figure 3. The vertical line at an area ratio of 1 indicates that there is obviously no discontinuity in pressure variation for a straight tube. It can be noted from the figure that the critical Knudsen number ($(Kn_j)_{cr}$, on the basis of smaller tube diameter) decreases with an increase in the area ratio. Interestingly, the figure suggests that discontinuity in slope is possible in the continuum regime as well for sufficiently large area ratios. The following correlation is formulated for $(Kn_j)_{cr}$ on the basis of the experimental data in figure 3:

$$(Kn_j)_{cr} = -3.122 \times 10^{-3} \log_e(AR) + 0.0131 \quad (1.48 \leqslant AR \leqslant 64). \tag{3.1}$$

Equation (3.1) fits the experimental data points within ±16 % range with a root-mean-square (r.m.s.) error of 3.5 %. The correlation indicates that the critical Knudsen number decreases logarithmically with an increase in the area ratio.

The absence of flow separation near the junction is another noticeable feature from these measurements; flow separation would manifest as an adverse pressure gradient, which is clearly absent in figure 2. The highest Reynolds number in these measurements is 837. These new and interesting observations are confirmed

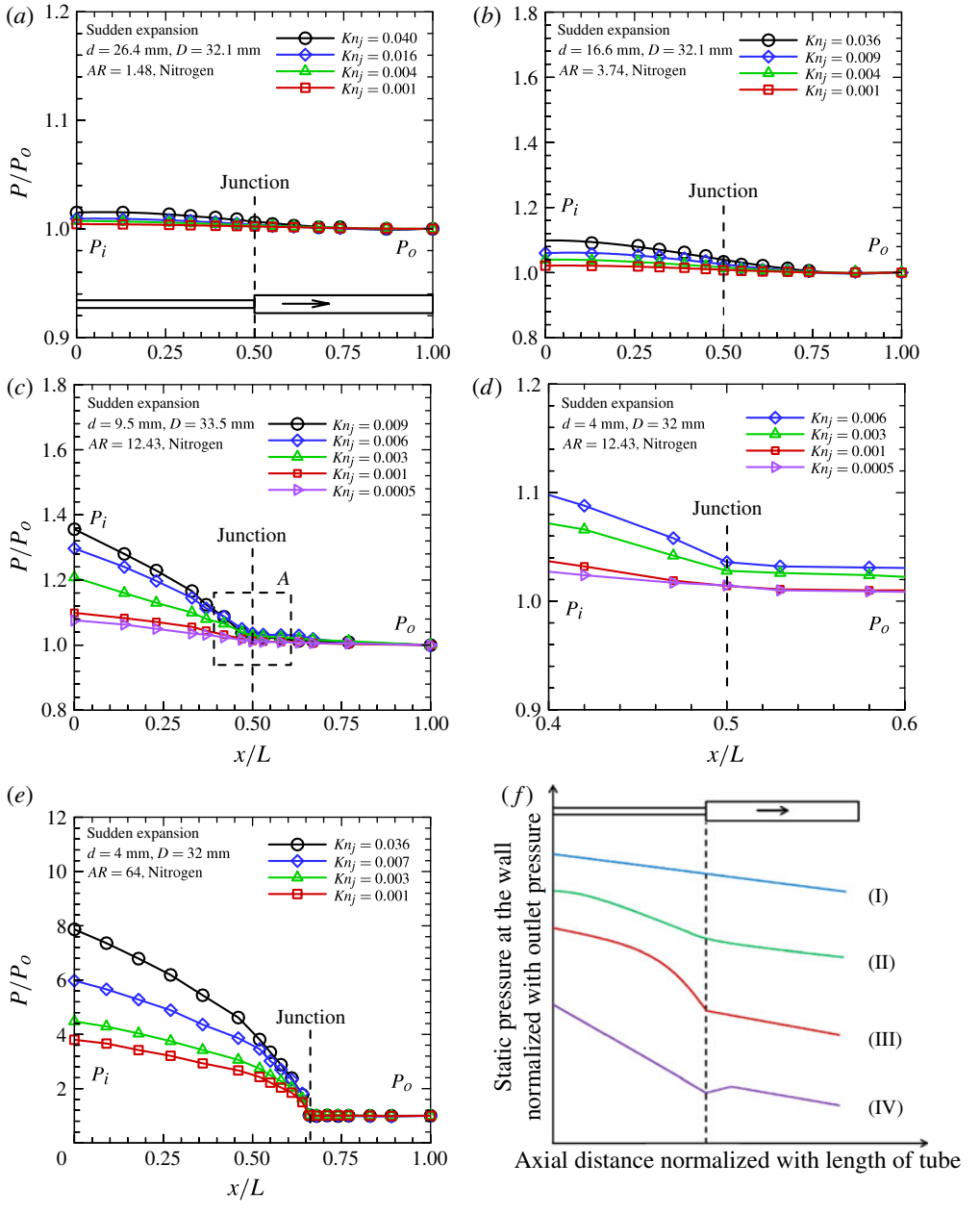

FIGURE 2. (Colour online) Static pressure variation (normalized with outlet pressure) along the wall: (*a*) $AR = 1.48$; (*b*) $AR = 3.74$; (*c*) $AR = 12.43$; (*d*) expanded view of *A* from $AR = 12.43$; (*e*) $AR = 64$; (*f*) schematic diagrams of static pressure variation at the wall of sudden expansion (I = low-*Re* continuum gas flow with low area ratio, II = low-pressure ratio rarefied gas flow (Lee *et al.* 2002), III = high-pressure ratio rarefied gas flow (Agrawal *et al.* 2005), IV = laminar liquid flow (Oliveira & Pinho 1997; Chalfi & Ghiaasiaan 2008)). (Here X = axial distance, m; L = length between first and last pressure tap, m; Kn_j = Knudsen number at junction; AR = area ratio, P_i = static pressure at the first pressure tap, P_o = static pressure at the last pressure tap.)

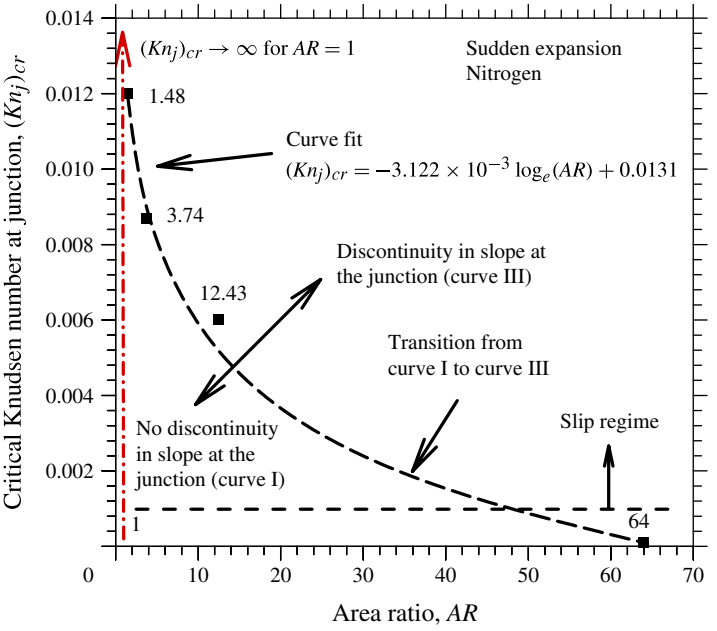

FIGURE 3. (Colour online) Effect of rarefaction and area ratio on discontinuity in the slope at the sudden expansion junction (labels along the curve indicate area ratio, refer to figure 2*f* for curves I, II and III; Kn_j is the Knudsen number at the junction on the basis of the smaller tube diameter).

by performing measurements at other values of Knudsen number. In addition to this, the static pressure at various radial locations just upstream and just downstream of the junction is measured for the four area ratios. The static pressure in the flow stream is normalized with the static pressure at the wall and plotted against the local radius normalized with the radius of the smaller section, as shown in figure 4. These static pressure measurements are observed to be within 4 % of the corresponding static pressure at the wall. In contrast, Oliveira & Pinho (1997) reported non-uniform radial pressure profiles just upstream and just downstream of the junction in the case of liquid flow with flow separation at the junction. The uniform radial pressure profiles just upstream and just downstream of the junction noted in the present work further indicate the absence of flow separation at the junction. The measurements were compared with numerical solution obtained using a commercial computational fluid dynamics (CFD) solver in the continuum regime. A maximum deviation of 10 % is observed in the local static pressure variation as compared with the numerical solution (not shown).

Agrawal *et al.* (2005) first reported the discontinuity in slope at the junction of a suddenly expanding microchannel, through their lattice-Boltzmann-method-based simulations. The simulations reported by Agrawal *et al.* (2005) are however for a planar geometry, and therefore cannot be compared quantitatively with the axisymmetric geometry results from the present experiments. Oliveira & Pinho (1997) however observed an adverse pressure gradient and flow reversal with liquid flow. The pressure variation reported by Oliveira & Pinho (1997) at $Re_s = 50$ is similar to curve IV in figure 2(*f*). Chalfi & Ghiaasiaan (2008) also noted a similar pressure variation in their study of continuum flows ($Re_s = 160$–$11\,000$). As is well known, the adverse pressure gradient downstream of the junction causes secondary flow at the junction for

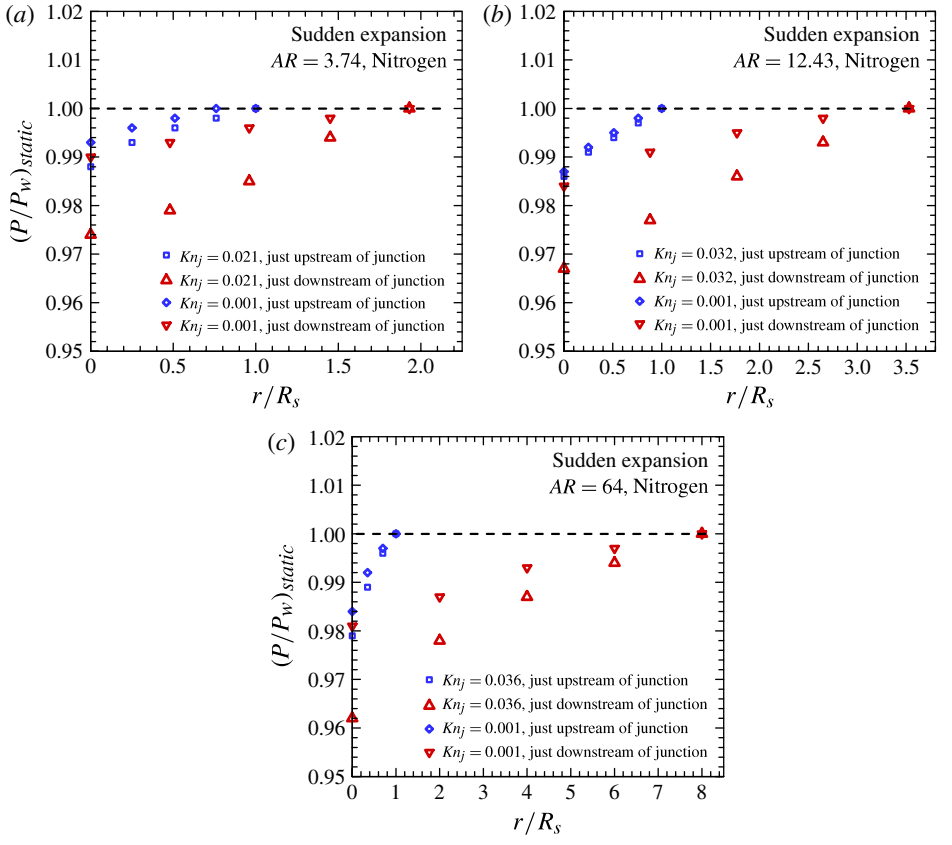

FIGURE 4. (Colour online) Radial static pressure variation just upstream and just downstream of the sudden expansion junction for (*a*) $AR = 3.74$, (*b*) $AR = 12.43$ and (*c*) $AR = 64$. Here, P is the local static pressure in the flow stream and P_w is the static pressure at the wall. r is radial distance from axis and R_s is radius of smaller section.

liquid flow through a sudden expansion. However, a dramatically different type of flow behaviour is noted here with rarefied gas flow through a sudden expansion.

3.2. *Effect of sudden expansion on pressure variation*

In this section, the pressure variation in each tube is individually compared with that of an isolated tube. The experimentally measured inlet pressure and the mass flow rate are used as inputs for computing the pressure variation in the isolated small tube, whereas the outlet pressure and the mass flow rate serve as inputs for computing the pressure variation in the isolated large tube. The pressure variation for the straight tube is computed from the analytical solution of Sreekanth (1969).

The comparison in pressure variation for a sudden expansion and isolated straight tubes is presented in figure 5 for one set of parameters. While the pressure variation between the two cases agree sufficiently far away from the junction, the pressure drops more rapidly for the sudden expansion case. The overall pressure drop is clearly larger for the tubes connected in series (sudden expansion case with area ratio of 3.74, 12.43 and 64) as compared with the two isolated tubes. However, for the area ratio of 1.48, the static pressure variation is same (maximum deviation of $+2\,\%$) as that for the isolated straight tubes. The result for the smallest area ratio therefore agrees

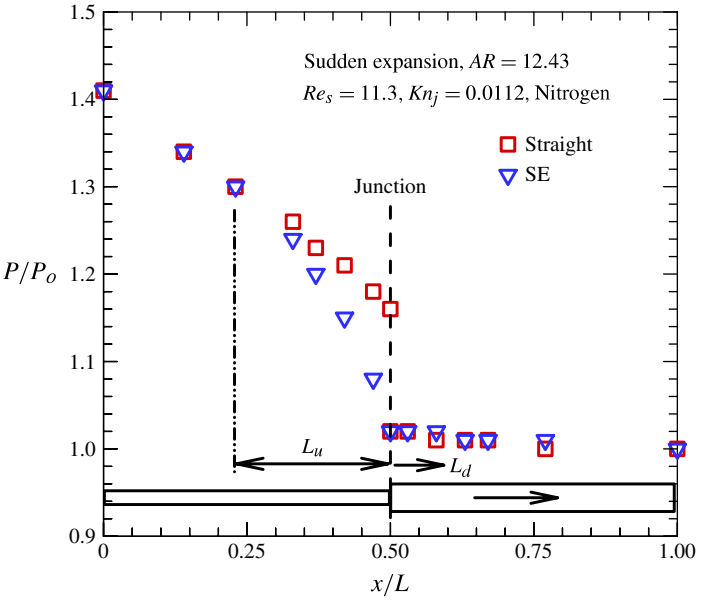

FIGURE 5. (Colour online) Static pressure variation (normalized with the outlet pressure) along the wall. Here $Re_s = Re$ in the smaller section, $Kn_j = Kn$ at the junction on the basis of the smaller tube diameter, X is the axial distance (m), L is the length of the tube (m) and SE is the sudden expansion.

qualitatively with the simulation results in Agrawal *et al.* (2005) with area ratio of two.

The distance (L_u) from the junction to the upstream point, where the difference in pressure between smaller section of sudden expansion and corresponding isolated straight tube first appears can be gleaned from figure 5. This distance normalized by the smaller tube diameter is plotted in figure 6 as a function of the Knudsen number at the junction. The figure shows that L_u is of the order of the tube diameter and increases monotonically with respect to the Knudsen number. A correlation (equation (3.2)) is formulated for L_u/d on the basis of the experimental data in figure 6:

$$\frac{L_u}{d} = 15.45(AR \times Kn_j)^{0.52} \quad (3.74 \leqslant AR \leqslant 64,\ 0.0005 \leqslant Kn_j \leqslant 0.062) \tag{3.2}$$

where d is the smaller tube diameter (m), AR is the larger section area/smaller section area ratio, Kn_j is the Knudsen number at the junction on the basis of smaller tube diameter. The correlation fits the experimental data points within $\pm 20\,\%$ range (2 data points out of 15 data points fall outside the range) with a r.m.s. error of $4.2\,\%$. The relatively large error could be because of the limited resolution in the measurements; the resolution is dictated by the spacing between the pressure taps. Equation (3.2) indicates that for a given area ratio, L_u/d varies approximately as the square root of the Knudsen number at the junction. The result suggests that the flow senses the presence of the junction much before reaching there, and begins to adjust its state. Further, the presence of the junction, as measured by the distance L_u, is felt over a longer distance upstream of the junction for a larger Knudsen number and a higher area ratio.

Similarly, the distance (L_d) from the junction to the downstream point where the difference in pressure between the larger tube of the sudden expansion and the

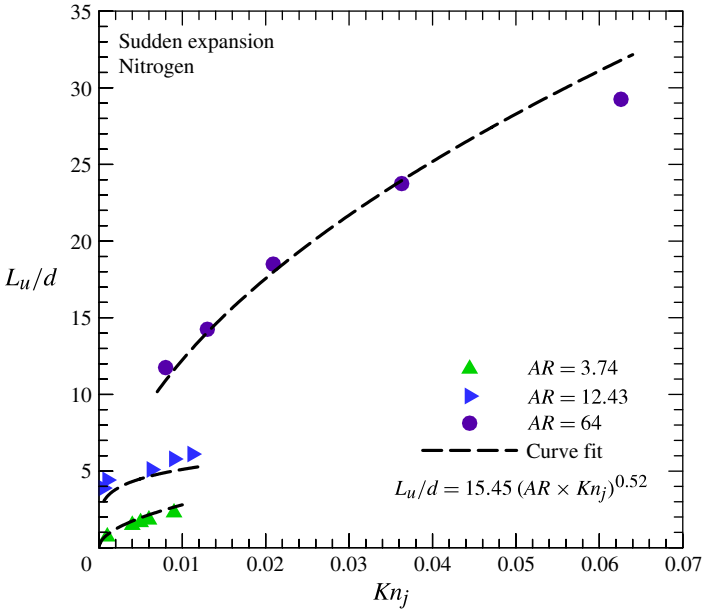

FIGURE 6. (Colour online) Variation in L_u (normalized with the smaller section tube diameter d) versus Knudsen number at the junction (Kn_j) on the basis of the smaller tube diameter. Here L_u is the length from the junction to the upstream point where the deviation in pressure between sudden expansion and the straight tube first appears.

corresponding isolated straight tube first appears is plotted in figure 7 as a function of the Knudsen number at the junction. The figure indicates that the distance L_d increases with an increase in area ratio, but decreases as Kn increases. The following correlation is proposed for L_d/d on the basis of the experimental data in figure 7:

$$\frac{L_d}{d} = \frac{AR^{1.35}}{400(Kn_j)^{0.45}} \quad (3.74 \leqslant AR \leqslant 64,\ 0.0005 \leqslant Kn_j \leqslant 0.062). \tag{3.3}$$

The correlation fits the experimental data points within $\pm 20\,\%$ range with a r.m.s. error of $3\,\%$. Again, the limited measurement resolution may be the reason for the relatively large error. The correlation indicates that for a given area ratio, L_d/d varies approximately as the square root inverse of the Knudsen number at the junction. Clearly the static pressure variation in the larger tube approaches the pressure variation as that of an isolated straight tube with an increase in rarefaction for a given area ratio. In contrast to the variation of L_u, the information about the presence of the junction is not propagated far downstream in the flow. The reason for this variation of L_u and L_d is discussed in § 4.1.

3.3. *Effect of sudden expansion on velocity distribution*

The objective of this section is to present the effect of sudden expansion on the velocity distribution in the two tubes. The following methodology is used for obtaining the velocity distribution for gas flow through a tube with sudden expansion. The velocity profile is assumed to be either a second-order or a fourth-order polynomial. Sreekanth (1969) through direct measurements showed that the velocity profile for rarefied gas flow in a tube is parabolic. That is, the velocity profile will be parabolic even for the present case far away from the junction (i.e. $x < L_u$, where x is the

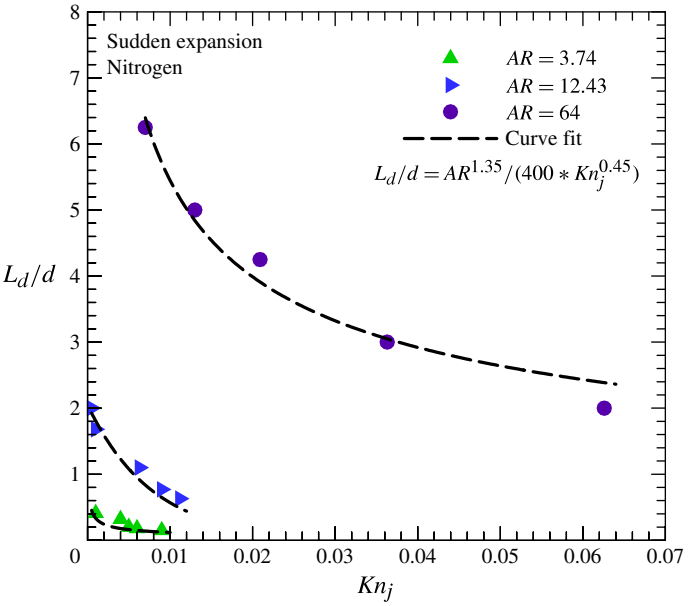

FIGURE 7. (Colour online) Variation in L_d (normalized with smaller section tube diameter d) versus Knudsen number at junction (Kn_j) on the basis of smaller tube diameter. Here L_d is the length from the junction to the downstream point where the deviation in pressure between the sudden expansion and the straight tube first appears.

streamwise coordinate). In the case of continuum flow, the distortion of the velocity profile from the parabolic shape near the sudden expansion junction was noted by Durst *et al.* (1974) and Oliveira & Pinho (1997). Therefore, considering the possibility that the sudden expansion can distort the velocity profile close to the junction ($L_u < x < L_d$), both second- and fourth-order polynomial velocity profiles were tested in our analysis. The fourth-order velocity profile was tested such that any distortion in the velocity profile near the junction will be reflected in its shape.

The parabolic profile is given by

$$u = a + br^2 \tag{3.4}$$

where a and b are coefficients to be determined and r is the radial coordinate. The mass flow rate (kg s^{-1}) is calculated as

$$\dot{m} = \int_0^R \rho 2\pi r \, \mathrm{d}ru \tag{3.5}$$

where ρ is the density of gas (kg m^{-3}) and R is the radius of the tube (m). The values of mass flow rate and gas density are obtained from experimental measurements. For rarefied gas flow through a tube, the slip velocity at the wall using second-order slip boundary condition (Cercignani 1964; Sreekanth 1969; Cercignani & Lorenzani 2010) is given by

$$u_s = -C_1\lambda\left(\frac{\partial u}{\partial r}\right)_{wall} - C_2\lambda^2\left(\frac{\partial^2 u}{\partial r^2}\right)_{wall} \tag{3.6}$$

where C_1 and C_2 are the first- and second-order slip coefficients, with $C_1 = 1.1466$ and $C_2 = 0.14$ (Sreekanth 1969; Agrawal & Prabhu 2008). By employing (3.5) and (3.6),

the values of coefficients a, b in (3.4) can be determined; and therefore the complete velocity distribution is known. It must be noted that both the coefficients are strong functions of the streamwise coordinate.

The velocity profile obtained from the above analysis can be verified by substituting it in the momentum equation. The integral form of the momentum equation for a finite size control volume (see figure 1*c*) is

$$(p_1 - p_2)A = \tau_w \pi d(x_2 - x_1) + [M_2 - M_1] \tag{3.7}$$

where p_1, p_2 is the static pressure (Pa) and M_1, M_2 is the momentum (N) at locations 1 and 2, respectively, τ_w is the average shear stress between locations 1 and 2 (N m^{-2}), d is the internal diameter (m) of the tube and A is the cross-sectional area (m^2) of the tube. Note that p_1, p_2, A, d, x_1 and x_2 are known from the experimental measurements. From the velocity profile (equation (3.4)), the shear stress at the wall (τ_w) and momentum M_1 and M_2 can readily be calculated from

$$\tau_w = \mu \left(\frac{\mathrm{d}u}{\mathrm{d}r} \right)_{r=R} \tag{3.8}$$

$$M = \int_0^R \rho 2\pi r \, \mathrm{d}r u^2 \tag{3.9}$$

where $\rho = p/(R_g T)$, p is the experimentally measured pressure (Pa), R_g is the specific gas constant (J (kg K)$^{-1}$), T is the temperature of the gas (K). The average shear stress at the wall for the control volume is calculated from τ_{w1}, τ_{w2} using (3.8) and (3.10); where τ_{w1}, τ_{w2} are the shear stress for points 1 and 2:

$$\tau_w = \frac{\tau_{w1} + \tau_{w2}}{2}. \tag{3.10}$$

The various terms calculated based on the velocity profile at locations 1 and 2 indeed satisfy the momentum equation. This observation applies to all control volumes starting from the first pressure tap to the junction, which justifies the assumption of a second-order parabolic velocity profile. It further suggests that the velocity slip model (equation (3.6)) is applicable in the present case. The analysis also helps in bringing out the relative contributions of the increase in momentum and increase in wall shear stress, in the overall pressure drop.

Considering the possibility that the sudden expansion can distort the velocity profile close to the junction ($L_u < x < L_d$), a fourth-order polynomial velocity profile (given below) was also tested:

$$u = a + br^2 + cr^4. \tag{3.11}$$

Note that due to symmetry consideration, the velocity profile is expected to be an even function of r, and therefore coefficients of r and r^3 terms have been set as zero. Considering the control volume with point 1 located just upstream of the point where difference in pressure variation of sudden expansion and that of an isolated straight tube begins to appear. The velocity distribution at point 1, which is parabolic, is known. The fourth-order velocity profile (equation (3.11)) is assumed at point 2, leaving three unknown coefficients to be determined. The three conditions used to evaluate the three coefficients are the slip condition at the wall (equation (3.6)), the mass flow rate (which is known) and the momentum equation (equation (3.7)). Once the fourth-order velocity profile was determined at point 2, the procedure can be extended for subsequent control volumes all of the way to the junction. It is observed

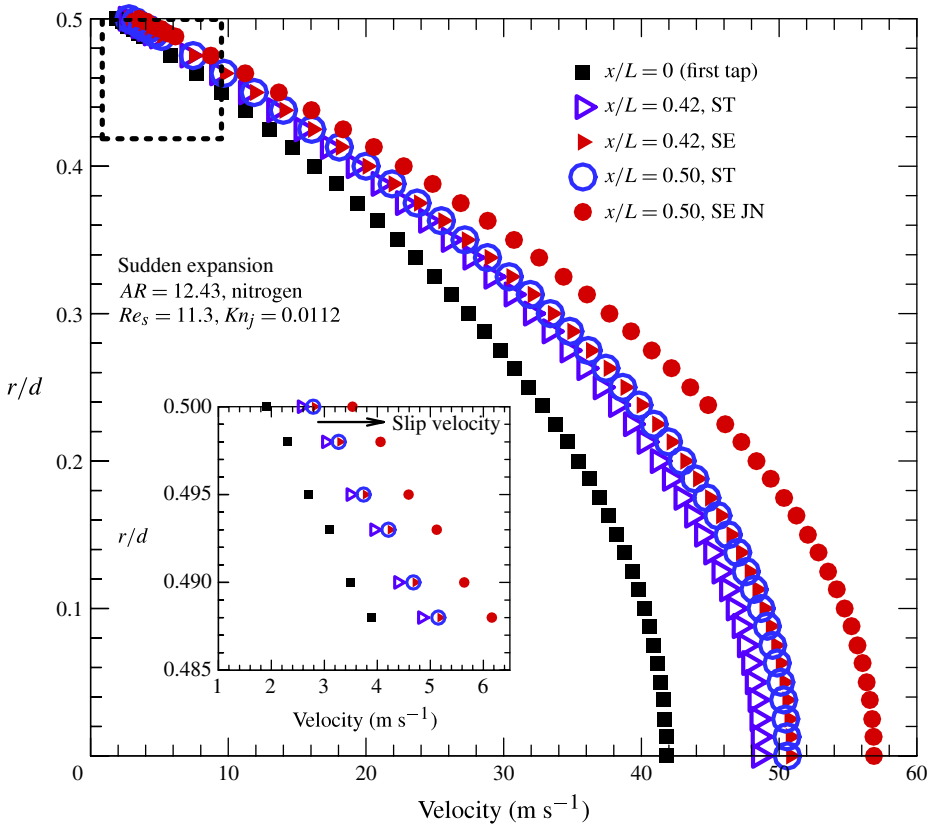

FIGURE 8. (Colour online) Velocity profile for the smaller section of the sudden expansion and the straight tube. Here $Re_s = Re$ in the smaller section, $Kn_j = Kn$ at the junction, ST is the straight tube, SE is the sudden expansion, JN is just upstream of the junction, X is the axial distance (m), L is the length of the tube (m), r is the local radius (m) and d is the internal diameter of the smaller tube (m).

that the fourth-order velocity profiles are same as the second-order velocity profiles even close to the upstream of the junction (i.e. the contribution of the last term in (3.11) is negligibly small); thereby confirming that the velocity profile is indeed parabolic throughout both the entire tubes.

Figure 8 presents the velocity profile in the smaller tube. The velocity distribution for an isolated straight tube (hereafter referred as 'straight' tube) is also plotted for comparison. The latter is available from the analytical solution of Sreekanth (1969). The velocity profiles from the first pressure tap to the junction are plotted in figure 8 for an area ratio of 12.43, for $Kn_j = 0.0112$ case. The velocity for the sudden expansion is greater than the straight tube owing to the lower density at that location in the former case. With reference to a straight tube, the increase in the central velocity for the sudden expansion case is observed to be larger towards the junction. The variation in the slip velocity is shown in figure 8; a higher amount of slip is noted with sudden expansion as compared with that for a straight tube.

Figure 9 shows the velocity profiles from the last pressure tap to the junction for an area ratio of 12.43, for the case $Kn_j = 0.0112$. The velocity for the sudden expansion

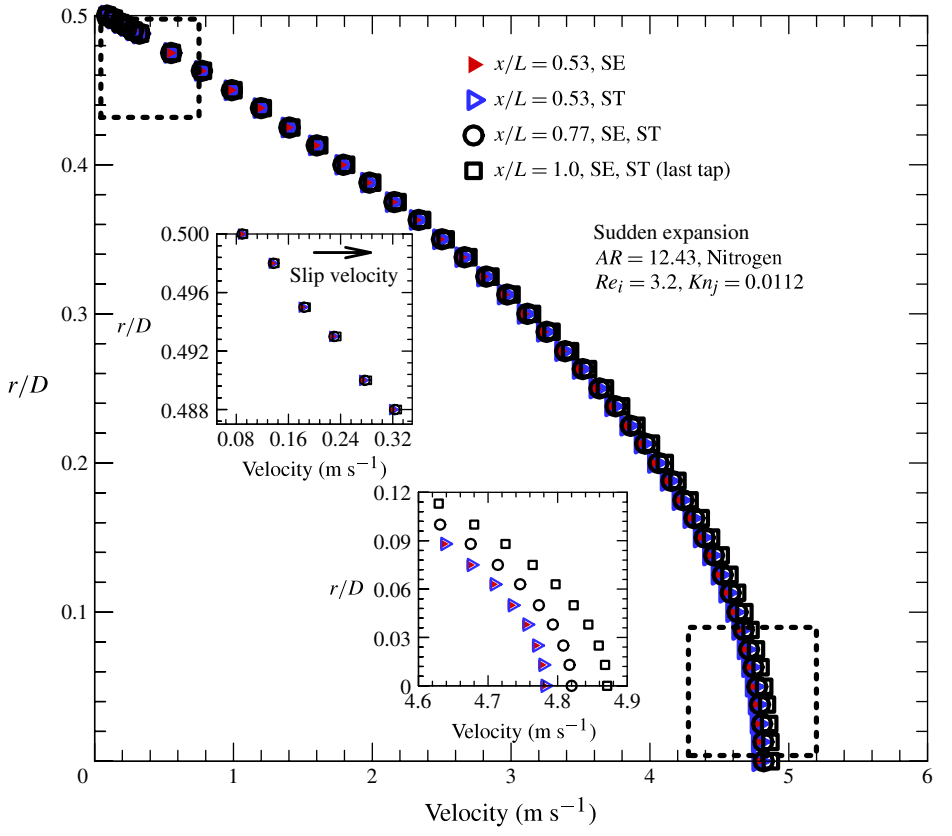

FIGURE 9. (Colour online) Velocity profile for larger section of sudden expansion and straight tube. Here $Re_l = Re$ in the larger section, $Kn_j = Kn$ at the junction, ST is the straight tube, SE is the sudden expansion, X is the axial distance (m), L is the length of the tube (m), r is the local radius (m) and D is the internal diameter of the larger tube (m).

is marginally lower than the straight tube near the junction owing to a lower density at that location in the straight tube case. Further downstream (at a distance L_d from the junction) the velocity profile in the larger tube is identical to that of the straight tube. The variation in the slip velocity is shown in figure 9; the same amount of slip is noted with sudden expansion as compared with that for a straight tube due to nearly constant velocity in the larger tube.

3.4. *The effect of sudden expansion on the wall shear stress and momentum*

The results in the previous section indicate that the distortion from the parabolic velocity profile upstream of the junction is not observed due to higher slip at the wall or acceleration of the flow. The parabolic second-order velocity profile therefore continues to be a justified assumption in the case of rarefied gas flow through sudden expansion. The calculated velocity profile is used to further evaluate the wall shear stress and flow momentum in this section.

The wall shear stress and the momentum for sudden expansion and a straight tube as a function of the axial location is shown in figures 10 and 11. The wall shear stress and momentum are identical for the two cases away from the junction. However, the sudden expansion case has a higher wall shear stress and axial momentum (as

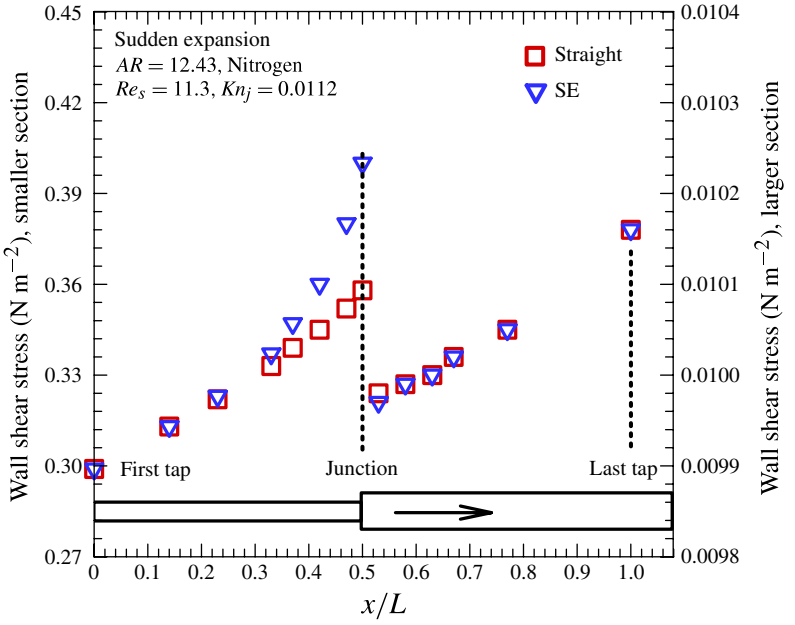

FIGURE 10. (Colour online) Wall Shear stress variation for sudden expansion and straight tube. Here $Re_s = Re$ in the smaller section, $Kn_j = Kn$ at the junction on the basis of the smaller tube diameter, SE is the sudden expansion, X is the axial distance (m) and L is the length of the tube (m).

compared with a straight tube) just upstream of the junction (figures 10 and 11). The increase in wall shear stress is owing to an increase in the velocity gradient at the wall. The extent of slip is larger in smaller tube of sudden expansion as shown in figure 8 and the velocity gradient at the wall is also higher for the same case. The wall shear stress and momentum in the larger tube are approximately the same as that of the straight tube (figures 10 and 11).

Figure 8 indicates that the central core of flow in the smaller tube of a sudden expansion is accelerated at a higher rate than the near-wall region, when compared with a straight tube. The rate of gas expansion in the central core increases as the junction is approached. The amount of velocity slip at the wall also increases; unlike conventional flows, where the flow has to satisfy the no-slip boundary condition at the wall. The rate of change of rarefaction up to the junction is directly proportional to the rate of gas expansion. The increased rarefaction causes an increase in the axial velocity, the wall shear stress and the momentum towards the junction as explained above. This results in increased pressure loss in the smaller section (analysed further in § 4).

The force balance for sudden expansion and the isolated straight tube is plotted in figure 12. The inlet flow condition and the geometry are the same for these cases. The pressure force is primarily balanced by viscous force away from the junction. The pressure force, shear force and inertia force in the larger tube are nearly same as that of the straight tube. The magnitude of the shear force is only marginally higher in the smaller tube of sudden expansion than that in the straight tube. The inertia force however increases rapidly in the smaller tube as compared with the straight tube, as the flow approaches the junction. The figure indicates that the flow acceleration due to the sudden expansion has a greater contribution in the overall pressure drop than

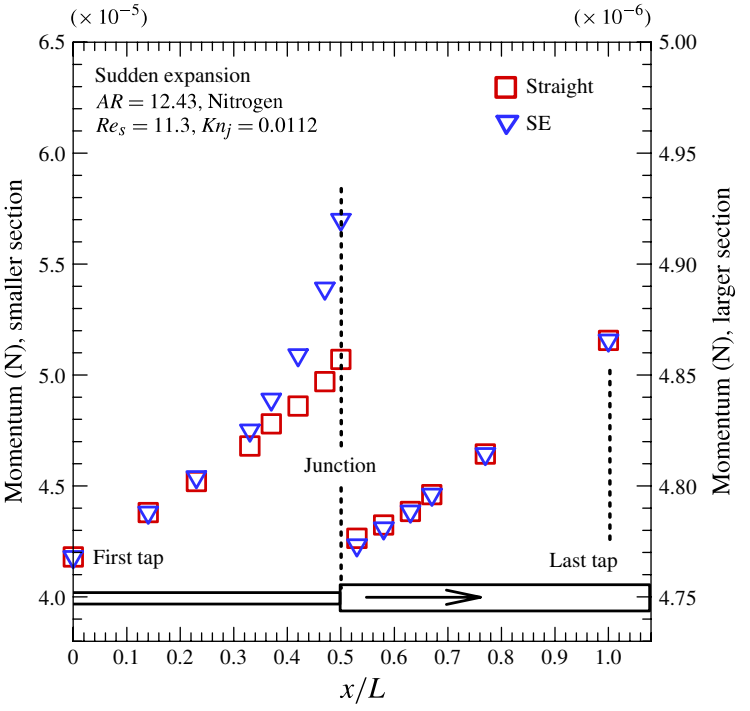

FIGURE 11. (Colour online) Momentum variation for sudden expansion and straight tube. Here $Re_s = Re$ in the smaller section, $Kn_j = Kn$ at the junction on the basis of the smaller tube diameter, SE is the sudden expansion, X is the axial distance (m) and L is the length of the tube (m).

the increase in the wall shear stress. The flow acceleration starts upstream away from the junction and leads to maximum velocity at the junction. This observation agrees qualitatively with the numerical simulations results of Xue & Chen (2003), Celik & Edis (2007) and Kursun & Kapat (2007).

3.5. *Effect of Kn and Re on the pressure loss coefficient*

The results in the previous sections provide information about the local variation in the pressure. The variation in pressure loss coefficient with Re and Kn from the overall pressure drop is discussed in this section. The overall pressure drop between the first and last pressure taps (refer figure 1*b*) for different mass flow rates (4 sccm (7.49×10^{-8} kg s^{-1}) to 4500 sccm (8.42×10^{-5} kg s^{-1})) is shown in figure 13. Note that the pressure drop with mass flow rate is plotted on log scale for the four test sections, in the figure. The pressure drop varies nonlinearly with mass flow rate similar to gas flow through uniform cross-section straight tube. However, the pressure drop is larger in the sudden expansion than that of the two isolated straight tubes, which is analysed further in § 4.2. The pressure drop is normalized with the dynamic pressure head at the inlet and presented in figure 14.

The pressure loss coefficient for the sudden expansion can be expressed in an analogous manner to that for incompressible flow as

$$K = \frac{\Delta P}{\frac{1}{2}\rho_i U_i^2} \tag{3.12}$$

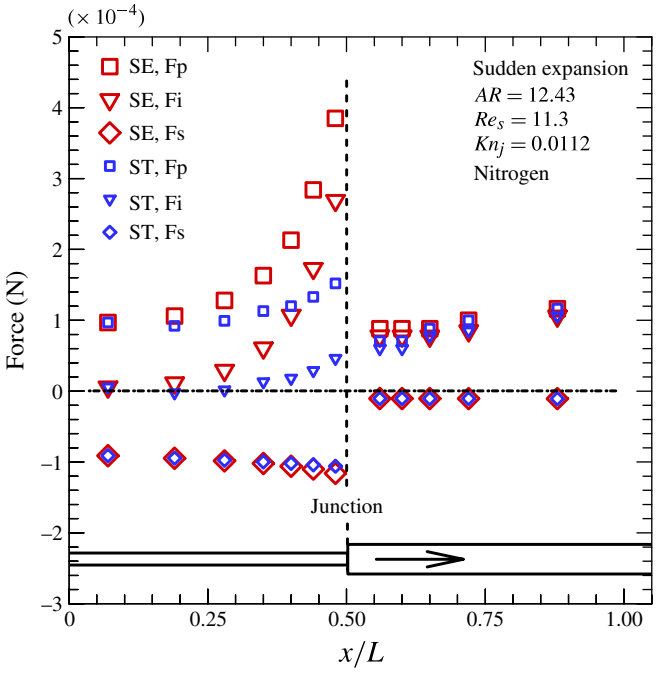

FIGURE 12. (Colour online) Force balance for sudden expansion and an isolated straight tube. Here $Re_s = Re$ in the smaller section, $Kn_j = Kn$ at the junction on the basis of the smaller tube diameter, ST is the straight tube, SE is the sudden expansion, *Fp* is the pressure force, *Fi* is the inertia force, *Fs* is the shear force, X is the axial distance (m) and L is the length of the tube (m).

where ΔP is the pressure drop between the first and the last pressure taps (Pa), ρ_i is the density of gas at the first pressure tap (kg m^{-3}) and U_i is the average velocity at the first pressure tap (m s^{-1}). The pressure loss coefficient is plotted in figure 14. The following correlation is proposed for K on the basis of the experimental data points:

$$K = \frac{692(AR)^{0.9}}{(1 + 183Kn_i) \times (Re_s)^{1.23}},$$
$$(1.48 \leqslant AR \leqslant 64,\ \ 0.0001 \leqslant Kn_i \leqslant 0.045,\ \ 0.20 \leqslant Re_s \leqslant 837). \qquad (3.13)$$

The correlation fits the experimental data points within $\pm 20\,\%$ range with a r.m.s. error of 1.3 %. Figure 14 shows the variation in $K(Re_s)^{1.23}$ with Kn_i. The figure indicates that K is a function of Kn, Re and area ratio in the slip regime. The correlation indicates that in the continuum regime ($Kn \to 0$), K is roughly independent of Kn and is primarily a function of the area ratio and Reynolds number.

4. Discussion

The reason for the increase in central velocity, wall shear stress and momentum towards the junction in the smaller tube is elaborated upon in this section. The larger pressure drop than the straight tube and the absence of flow separation at the junction are also discussed.

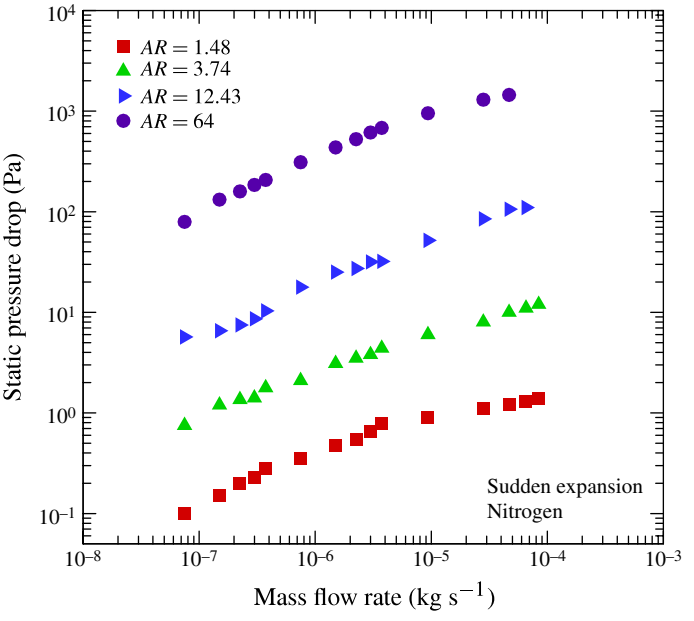

FIGURE 13. (Colour online) Static pressure drop in sudden expansion (AR = area ratio).

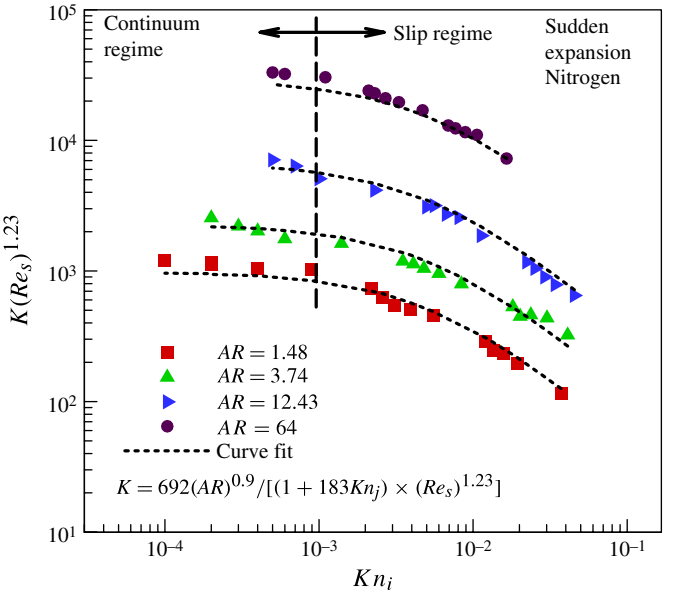

FIGURE 14. (Colour online) Variation in $K(Re_s)^a$ with Kn_i for sudden expansion (Re_s = 0.2–837, Knudsen number at the first tap, $Kn_i = 0.0001$–0.045, Mach number range at inlet, $M_i = 0.005$–0.26, AR = area ratio).

4.1. *The absence of flow separation at the junction*

The absence of an adverse pressure gradient at the junction is noted from figure 2, which indicates an absence of flow separation. It is in line with the numerical simulation results of Agrawal *et al.* (2005). Liou & Lin (2013) reported the absence of flow separation for low Reynolds number ($Re = 3.6$, Kn at outlet $= 0.1$) in a numerical study on rarefied gas flow through microchannel with a sudden contraction–expansion of 2:1:2 using an isothermal lattice Boltzmann method. However, in a numerical study (Darbandi & Roohi 2011) of rarefied gas flow, the flow separation is noted at the backward facing step of the microchannel (expansion ratio $= 2$, pressure ratio along the channel $= 2$). Alexeenko, Gimelshein & Levin (2005) observed separation in the transition section from their DSMC results with fully diffused gas–surface interaction, in their study of a microchannel with constriction (expansion ratio $= 4$, pressure ratio along the channel $= 2.47$). It was however mentioned that such a small separation region does not have any significant effect on the pressure drop and the pressure distribution along the microchannel. Alexeenko *et al.* (2005) further noted the absence of flow separation with specular gas–surface interaction, with low flow Mach number in the upstream channel. The simulations reported in the above-mentioned studies are for a two-dimensional geometry, and therefore cannot be compared quantitatively with the axisymmetric geometry results from the present experiments. The absence of flow separation is qualitatively in line with the above discussed simulations for low pressure ratio and low area ratio. Although no adverse pressure gradient has been observed in this work (pressure ratio < 1.4 for $AR \leqslant 12.43$), the possibility of a small separation region at the junction (in such a magnitude that it does not substantially affects the pressure distribution), as noted by Alexeenko *et al.* (2005), cannot be ruled out altogether.

In contrast, flow separation at the junction is observed with liquid flow (Oliveira & Pinho 1997; Chalfi & Ghiaasiaan 2008). The difference in liquid and gas flow behaviour is explained as follows. In case of gas flow (in the considered regime), the kinetic energy (KE) of the gas flow is negligible as compared with the driving pressure energy of the flow (Lee *et al.* 2002). The KE of the flow reduces at the junction due to sudden enlargement of the cross-section. This reduction in KE is so small that no significant effect on the pressure variation is observed. Therefore, no adverse pressure gradient at the junction is observed and the flow separation gets delayed/suppressed altogether in case of low Re continuum and slip flow regime. In the case of liquids, the KE is comparable with that of pressure energy even for low Re flow. The drop in KE at the junction causes an increase in the pressure just downstream of the junction resulting in an adverse pressure gradient and secondary flows at the corner of the junction with liquid flow. Macagno & Hung (1967) noted a small corner eddy for liquid flow through circular conduit sudden expansion with a low Reynolds number ($Re_s = 1$) in a smaller tube.

The absence of flow separation at the junction for a low Re continuum gas flow regime to a slip flow regime can also be understood from the point of view of momentum diffusion. The momentum diffusion, involving product of μ/ρ and second gradient of velocity, is proportional to kinematic viscosity. The momentum diffusivity increases in the case of rarefied gas flow to a large extent due to rarefaction, as compared with continuum flow. The flow is therefore subjected to larger radial momentum diffusion at the junction. In this kinetic environment, as the gas enters the larger tube just downstream of the junction, the gas molecules find way in the radial direction as well; Rathakrishnan & Sreekanth (1995) termed this as the relief effect. The streamlines near the sudden expansion junction for an area ratio of 12.43

are plotted in figure 15(*a*) using the velocity distribution discussed in § 3.3. It can be noted from the figure that the streamlines are of concave pattern and curved in the radial direction just downstream of the junction; indicating gas motion in the radial direction. Since the gas molecules leaving the smaller tube at the junction follow the surface in the radial direction (figure 15*a,b*), there is no secondary flow at the junction. Having finite momentum at the wall (due to slip) further helps in preventing the secondary flow. In contrast, the streamlines in case of incompressible flow exhibit a convex pattern (Oliveira & Pinho 1997), depicted schematically in figure 15(*c*). Larger radial momentum diffusion leads to a smaller value of L_d downstream of the junction. This explanation is therefore in line with the observation in figure 7.

In addition to above-mentioned points, the absence of flow separation can also be deduced from only marginal deviation in the velocity profile just downstream of the junction as compared with the straight tube (figure 9). Further, the wall shear stress and momentum in the larger tube are approximately the same as that of a straight tube (figures 10 and 11). Also, the pressure force, shear force and inertia force in the larger tube are nearly the same as that of a straight tube (figure 12).

The rarefied gas flow is also subjected to a large axial momentum diffusion upstream of the junction, due to rarefaction and larger axial gradient of streamwise velocity (as evident from figure 5); as compared with its continuum counterpart or rarefied flow in a straight tube. Thus, any distortion in the flow imposed by the sudden expansion travels backwards into the flow due to the large axial momentum diffusivity, and the flow starts adjusting itself sufficiently upstream. Here it is the viscous diffusion that contributes more in adjusting the flow upstream of the expansion, as also mentioned by Oliveira & Pinho (1997). This hypothesis is supported by the calculation of L_u, which indeed exhibits a systematic variation with rarefaction and area ratio (figure 6). The systematic variation in L_u suggests that the gas flow exhibits a 'predictive memory' because of the larger axial momentum diffusion. The approximately square-root dependence of L_u/d (and L_d/d) on Kn_j (see (2.5) and (2.6)) lends further credence to the hypothesis. The fact that there is finite slip velocity at the walls exaggerates this predictive memory effect.

4.2. *Larger pressure drop than isolated straight tube*

It is observed from figure 5 that the overall pressure drop in sudden expansion is larger than the pressure drop for straight tubes considered separately under the same flow conditions as that of a sudden expansion. This is apparently surprising because there are no secondary losses near the junction, as already noted from figures 2 and 4. In the velocity analysis (figure 8), it is observed that the central core of the flow accelerates up to the sudden expansion junction more than that of a straight tube flow for the same inlet flow condition. It is noted that this higher acceleration causes a larger pressure drop in the smaller tube than that of straight tube, as evident from figure 5. This gas flow expansion causes additional acceleration of the flow in the smaller tube, over and above what would be observed in a straight tube. The gas flow expansion however does not happen suddenly at the junction although there is a sudden increase in the cross-sectional area. As discussed above, the expansion starts upstream away from the junction and then continues gradually with a nonlinear pressure variation up to the junction. However, a jump in average velocity is observed at the junction from figures 8 and 9 due to the sudden increase in the cross-sectional area (see also Agrawal *et al.* 2005) and a larger momentum diffusion at the junction. Considering all of these effects, the total pressure drop in the smaller section can be separated as follows.

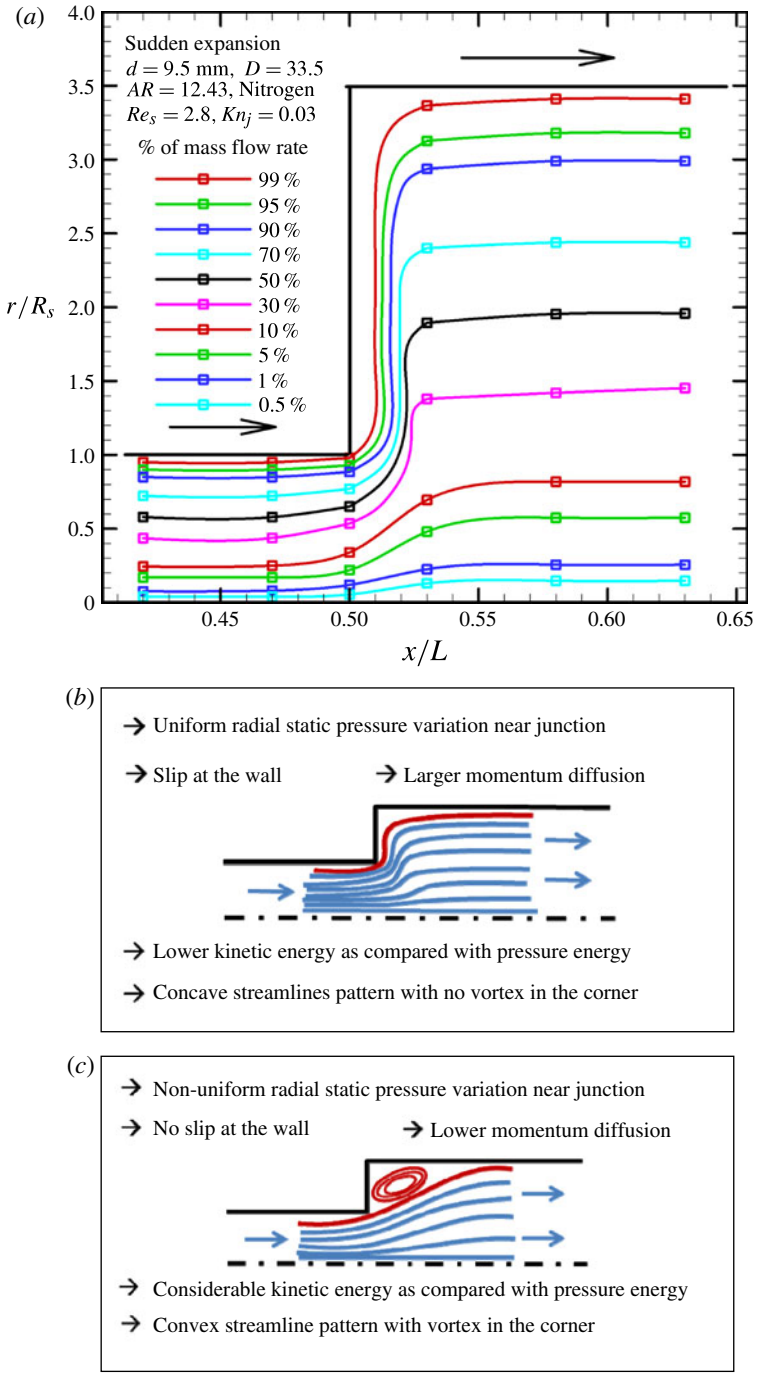

FIGURE 15. (Colour online) (*a*) Streamlines near the sudden expansion junction for rarefied gas flow. Here r is radial distance from axis and R_s is radius of smaller section. (*b*) Schematic streamlines of rarefied gas flow near the junction. (*c*) Schematic streamlines of laminar, incompressible, separated flow (Oliveira & Pinho 1997; Lee *et al.* 2002) near the junction.

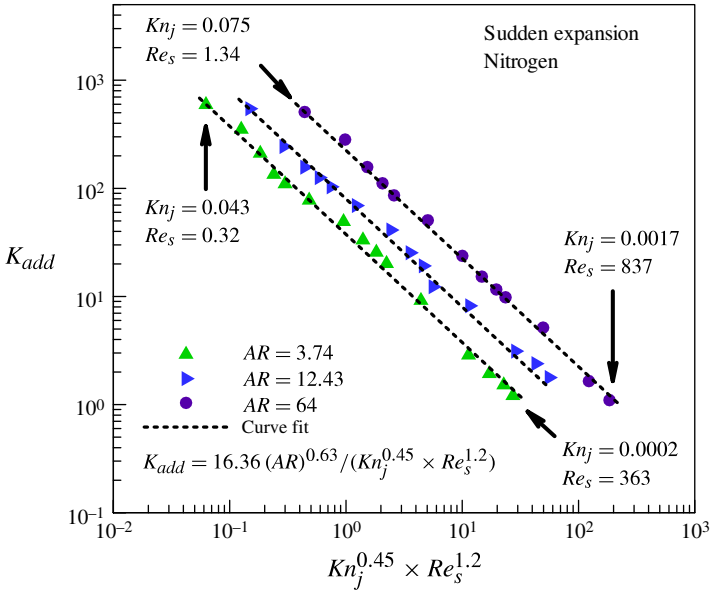

FIGURE 16. (Colour online) Variation in K_{add} with $(Kn_j^{0.45} \times Re_s^{1.2})$ for sudden expansion $(K_{add} = (\Delta p)_{add}/(0.5\rho_j U_j^2)$, $Re_s = Re$ in smaller section, $Kn_j = Kn$ at the junction on the basis of the smaller tube diameter and AR is the area ratio).

Total pressure drop in the smaller section = frictional pressure drop in the straight tube + acceleration pressure drop in the straight tube + additional acceleration pressure drop due to sudden expansion + additional frictional pressure drop from the acceleration due to sudden expansion.

The additional pressure drop (ΔP_{add}) in the sudden expansion is obtained by subtracting pressure drop in the isolated straight tubes from the sudden expansion pressure drop. The additional pressure loss coefficient for the sudden contraction can be expressed as

$$K_{add} = \frac{\Delta P_{add}}{\frac{1}{2}\rho_j U_j^2} \tag{4.1}$$

where ΔP_{add} is the additional pressure drop (Pa) ρ_j is the density of gas at the junction (kg m^{-3}) and U_j is the average velocity at the junction on the basis of the smaller section area of sudden expansion (m s^{-1}). The additional pressure loss coefficient as a function of $[(Kn_j)^a \times (Re_s)^b]$ is presented in figure 16. The following correlation is proposed for K_{add} on the basis of experimental data in figure 16:

$$K_{add} = \frac{16.36(AR)^{0.63}}{(Kn_j)^{0.45} \times (Re_s)^{1.2}},$$
$$(3.74 \leqslant AR \leqslant 64,\ 0.0002 \leqslant Kn_j \leqslant 0.075,\ 0.32 \leqslant Re_s \leqslant 837). \tag{4.2}$$

The correlation fits the experimental data points within ±20 % range with a r.m.s. error of 2.4 %. The correlation indicates that the normalized additional pressure drop is proportional to area ratio. For a given area ratio, K_{add} varies inversely with $(Kn_j)^{0.45}$

and $(Re_s)^{1.2}$. The correlation for L_u (equation (3.2)) and L_d (equation (3.3)) can be useful in estimating the location of pressure measurements taps for direct measurement of additional pressure drop for sudden expansion.

5. Conclusions

Rarefied gas flow experiments are carried out for four test sections of circular cross-section with a sudden expansion (area ratios of 1.48, 3.74, 12.43 and 64) in the slip flow regime ($0.0001 < Kn < 0.075$; $0.2 < Re_s < 837$). The static pressure along the wall is measured and analysed to understand the flow physics. The velocity profile is obtained by applying momentum balance and using experimental mass flow rate and pressure measurements at the wall. These results are compared with the solutions obtained for a straight tube of the same diameter and length following a similar analysis.

An adverse pressure gradient is not observed close to the junction in any of the cases investigated, suggesting the absence of flow separation. The overall pressure drop is however still larger with sudden expansion as compared with isolated tubes in series; this surprising observation is owing to an increased acceleration of the flow in the sudden expansion case. The measurements suggest that the gas flow expansion does not happen suddenly although there is a sudden increase in the cross-sectional area at the junction. In fact, the expansion starts upstream away from the junction and continues gradually with a nonlinear pressure variation up to the junction; this expansion of the gas is aided by velocity slip at the wall. The upstream distance from the junction, where this additional acceleration begins, increases with an increase in the Knudsen number; this is related to increased axial momentum diffusion in rarefied gas flow. The downstream distance from the junction beyond which the additional acceleration ceases however reduces with an increase in the Knudsen number, owing to an increased radial momentum diffusion. This additional acceleration of the flow increases the velocity gradient at the wall leading to an increase in the axial momentum and wall shear stress near the junction. The force balance brings out the importance of inertia terms for this flow; the inertia force contributes substantially in the overall pressure drop, while the relative contribution of the wall shear stress diminishes close to the junction.

Our analysis suggests that the velocity profile remains parabolic throughout both the entire tubes. Interestingly, the pressure variation is significantly different from its continuum counterpart. A discontinuity in the slope of streamwise variation of pressure appears at the junction beyond a critical value of the Knudsen number; the critical value of Knudsen number is a strong function of the expansion area ratio. The pressure loss coefficient is a function of Kn, Re and the area ratio in the slip flow regime.

It is proposed that rarefied gas flow exhibits a predictive memory because of the larger axial momentum diffusion. This makes the flow behaviour at microscale/rarefied gas flow dramatically different from their continuum counterpart; in that the flow senses the oncoming expansion junction earlier and accordingly starts adjusting to the change in the cross-section area. These novel results should help improve our understanding of rarefied gas flow and gas flow in complex microchannels.

Acknowledgements

The authors acknowledge financial support for this work from the Indian Space Research Organization and IIT Bombay.

REFERENCES

ABDELALL, F. F., HAHN, G, GHIAASIAAN, S. M., ABDEL-KHALIK, S. I., JETER, S. S., YODA, M. & SADOWSKI, D. L. 2005 Pressure drop caused by abrupt flow area changes in small channels. *Exp. Therm. Fluid Sci.* **29**, 425–434.

AGRAWAL, A. 2011 A comprehensive review of gas flow in microchannels. *Intl J. Micro-Nanoscale Transport* **2** (1), 1–40.

AGRAWAL, A. & AGRAWAL, A. 2006 Three-dimensional simulation of gaseous slip flow in different aspect ratio microducts. *Phys. Fluids* **18**, 103604.

AGRAWAL, A., DJENIDI, L. & ANTONIA, R. A. 2005 Simulation of gas flow in microchannels with a sudden expansion or contraction. *J. Fluid Mech.* **530**, 135–144.

AGRAWAL, A. & PRABHU, S. V. 2008 Survey on measurement of tangential momentum accommodation coefficient. *J. Vacuum Sci. Technol.* A **26**, 634–645.

ALEXEENKO, A. A., GIMELSHEIN, S. F. & LEVIN, D. A. 2005 Reconsideration of low Reynolds number flow through constriction microchannels using the DSMC method. *J. Microelctromech. Syst.* **14**, 847–856.

ARKILIC, E. B., SCHIMIDT, M. A. & BREUER, K. S. 1997 Gaseous slip flow in long micro-channels. *J. Microelectromech. Syst.* **6**, 167–178.

BARBER, R. W. & EMERSON, D. R. 2001 A numerical investigation of low Reynolds number gaseous slip flow at the entrance of circular and parallel plate microchannels. *ECCOMAS Computational Fluid Dynamics Conference Swansea, Wales, UK, 4–7 September* 2001. European Community on Computational Methods in Applied Sciences.

CELIK, B. & EDIS, F. O. 2007 Computational investigation of micro backward-facing step duct flow in slip regime. *Nanoscale Microscale Thermophys. Engng* **11**, 319–331.

CERCIGNANI, C. 1964 Higher-order slip according to the linearized Boltzmann equation. rep. AS64-19, Institute of Engineering Research, Berkeley.

CERCIGNANI, C. & LORENZANI, S. 2010 Variational derivation of second-order slip coefficients on the basis of the Boltzmann equation for hard-sphere molecules. *Phys. Fluids* **22**, 062004.

CHALFI, T. Y. & GHIAASIAAN, S. M. 2008 Pressure drop caused by flow area changes in capillaries under low flow conditions. *Intl J. Multiphase Flow* **34**, 2–12.

CHEN, R. Y. 1973 Flow in the entrance region at low Reynolds numbers. *Trans. ASME: J. Fluids Engng* **95**, 153–158.

DAGTEKIN, I. & UNSAL, M. 2011 Numerical analysis of axisymmetric and planer sudden expansion flows for laminar regime. *Intl J. Numer. Meth. Fluids* **65**, 1133–1144.

DARBANDI, M. & ROOHI, E. 2011 DSMC simulation of subsonic flow through nanochannels and micro/nano backward-facing steps. *Intl Commun. Heat Mass Transfer* **38**, 1443–1448.

DEMSIS, A., PRABHU, S. V. & AGRAWAL, A. 2010 Influence of wall condition on friction factor for flow of gases under slip condition. *Exp. Therm. Fluid Sci.* **348**, 1448–1455.

DEMSIS, A., VERMA, B, PRABHU, S. V. & AGRAWAL, A. 2009 Experimental determination of heat transfer coefficient in the slip regime and its anomalously low value. *Phys. Rev.* E **80**, 016311.

DOMBROWSKI, N., FOUMENY, E. A., OOKAWARA, S. & RIZA, A. 1993 The influence of Reynolds number on the entry length and pressure drop for laminar pipe flow. *Can. J. Chem. Engng* **71**, 472–476.

DONGARI, N., AGRAWAL, A. & AGRAWAL, A. 2007 Analytical solution of gaseous slip flow in long microchannels. *Intl J. Heat Mass Transfer* **50**, 3411–3421.

DURST, F., MELLING, A. & WHITELAW, J. H. 1974 Low Reynolds number flow over a plane symmetric sudden expansion. *J. Fluid Mech.* **641**, 111–128.

DURYODHAN, V. S., SINGH, S. G. & AGRAWAL, A. 2013 Liquid flow through a diverging microchannel. *Microfluid Nanofluid* **14**, 53–67.

EWART, T., PERRIER, P., GRAUR, I. A. & MEOLANS, J. G. 2006 Mass flow rate measurements in gas microflows. *Exp. Fluids* **41**, 487–498.

EWART, T., PERRIER, P., GRAUR, I. A. & MEOLANS, J. G. 2007 Mass flow rate measurements in a microchannel, from hydrodynamic to near free molecular regimes. *J. Fluid Mech.* **584**, 337–356.

FRIEDMANN, M, GILLIS, J. & LIRON, N. 1968 Laminar flow in a pipe at low and moderate Reynolds numbers. *Appl. Sci. Res.* **19**, 426–438.

GOHARZADEH, A. & RODGERS, P. 2009 Experimental measurement of laminar axisymmetric flow through confined annular geometries with sudden inward expansion. *J. Fluids Engng* **131**, 124501.

HAMMAD, K. J., OTUGEN, M. V. & ARIK, E. B. 1999 A PIV study of the laminar axisymmetric sudden expansion flow. *Exp. Fluids* **26**, 266–272.

HARLEY, J., HUANG, Y., BAU, H. & ZEMEL, J. N. 1995 Gas flow in microchannels. *J. Fluid Mech.* **284**, 257–274.

KURSUN, U. & KAPAT, J. S. 2007 Modelling of microscale gas flows in transition regime part I: flow over backward facing steps. *Nanoscale Microscale Thermophys. Engng* **11**, 15–30.

LEE, W. Y, WONG, M. & ZOHAR, Y. 2002 Microchannels in series connected via a contraction/expansion section. *J. Fluid Mech.* **459**, 187–206.

LIOU, T. M. & LIN, C. T. 2013 Study on microchannel flows with a sudden contraction–expansion at a wide range of Knudsen number using lattice Boltzmann method. *Microfluid Nanofluid* doi:10.1007/s10404-013-1200-2.

MACAGNO, E. O. & HUNG, T. K. 1967 Computational and experimental study of a captive annular eddy. *J. Fluid Mech.* **28** (1), 43–64.

MORINI, G. L., LORENZINI, M. & SALVIGNI, S. 2006 Friction characteristics of compressible gas flows in microtubes. *Exp. Therm. Fluid Sci.* **30** (8), 733–744.

OLIVEIRA, P. J. & PINHO, F. T. 1997 Pressure drop coefficient of laminar Newtonian flow in axisymmetric sudden expansions. *Intl J. Heat Fluid Flow* **18**, 518–529.

PAN, C. T., CHUANG, H. S., CHENG, C. Y. & YANG, C. T. 2004 Micro-flow measurement with a laser diode micro-particle image velocimetry. *Sensors Actuators* A **116**, 51–58.

PITAKARNNOP, J., VAROUTIS, S., VALOUGEORGIS, D., GEOFFROY, S., BALDAS, L. & COLIN, S. 2010 A novel experimental setup for gas microflows. *Microfluid Nanofluid* **8**, 57–72.

PONG, K., HO, C., LIU, J. & TAI, Y. 1994 Non-linear pressure distribution in uniform microchannels. *Appl. Microfabrication Fluid Mech.* **197**, 51–56.

RATHAKRISHNAN, E. & SREEKANTH, A. K. 1995 Rarefied flow through sudden enlargements. *Fluid Dyn. Res.* **16**, 131–145.

ROOHI, E. & DARBANDI, M. 2009 Extending the Navier–Stokes solutions to transition regime in two-dimensional micro- and nanochannel flows using information preservation scheme. *Phys. Fluids* **21**, 082001.

SHARIPOV, F. & SELEZNEV, V. 1998 Data on internal rarefied gas flows. *J. Phys. Chem. Ref. Data* **27** (3), 657–706.

SINGH, N., DONGARI, N. & AGRAWAL, A. 2013 Analytical solution of plane Poiseuille flow within Burnett hydrodynamics. *Microfluid Nanofluid* doi:10.1007/s10404-013-1224-7.

SISAWATH, S., JING, X., PAIN, C. C. & ZIMMERMAN, R. W. 2002 Creeping flow through an axisymmetric sudden contraction or expansion. *J. Fluids Engng* **124**, 273–278.

SREEKANTH, A. K. 1969 Slip flow through long circular tubes. In *Proceedings of the Sixth International Symposium on Rarefied Gas Dynamics* (ed. L. Trilling & H. Y. Wachman), pp. 667–680. Academic.

TSAI, C. H., CHEN, H. T., WANG, Y. N., LIN, C. H. & FU, L. M. 2007 Capabilities and limitations of 2-dimensional and 3-dimensional numerical methods in modelling the fluid flow in sudden expansion microchannels. *Microfluid Nanofluid* **3**, 13–18.

VERMA, B., DEMSIS, A., AGRAWAL, A. & PRABHU, S. V. 2009 Semiempirical correlation for the friction factor of gas flowing through smooth microtubes. *J. Vac. Sci. Technol.* A **273**, 584–590.

VIJAYALAKSHMI, K., ANOOP, K. B., PATEL, H. E., HARIKRISHNA, P. V., SUNDARARAJAN, T. & DAS, S. K. 2009 Effects of compressibility and transition to turbulence on flow through microchannels. *Intl J. Heat Mass Transfer* **52**, 2196–2204.

WENG, C. I., LI, W. L. & HWANG, C. C. 1999 Gaseous flow in microtubes at arbitrary Knudsen numbers. *Nanotechnology* **10**, 373–379.

XUE, H. & CHEN, S. 2003 DSMC simulation of microscale backward-facing step flow. *Microscale Thermophys. Engng* **7**, 69–86.

YAMAGUCHI, H., HANAWA, T., YAMAMOTO, O., YU, M., EGAMI, Y. & NIIMI, T. 2011 Experimental measurement on tangential momentum accommodation coefficient in a single microtube. *Microfluid Nanofluid* **11**, 57–64.

YANG, C.-Y., CHEN, C.-W, LIN, T.-Y. & KANDLIKAR, S. G. 2012 Heat transfer and friction characteristics of air flow in microtubes. *Exp. Therm. Fluid Sci.* **37**, 12–18.

ZOHAR, Y., LEE, S. Y. K., LEE, W. Y., JIANG, L. & TONG, P. 2002 Subsonic gas flow in a straight and uniform microchannel. *J. Fluid Mech.* **472**, 125–151.